

Solvatochromic Effects on the Electron Exchange Chemiluminescence (CIEEL) of Spiroadamantyl-Substituted Dioxetanes and the Fluorescence of Relevant Oxyanions[†]

Waldemar Adam,[‡] Irena Bronstein,[§] and Alexei V. Trofimov^{*,‡,‡,‡}

Institute of Organic Chemistry, University of Würzburg, Am Hubland, D-97074 Würzburg, Germany, Tropix, Inc., 47 Wiggins Avenue, Bedford, Massachusetts 01730, and Institute of Biochemical Physics, United Institute of Chemical Physics, Russian Academy of Sciences, ul. Kosygina 4, Moscow 117977, Russia

Received: September 16, 1997; In Final Form: March 11, 1998

A comparative spectral study on the intramolecular chemically initiated electron exchange luminescence (CIEEL) of five spiroadamantyl-substituted dioxetanes by various enzymatic and chemical triggers (alkaline phosphatase, HO⁻, and F⁻) in protic (H₂O, D₂O, and MeOH) and aprotic (MeCN and DMSO) solvents and the fluorescence of the authentic methyl *m*-oxybenzoate anion in the same media is reported. The present study reveals that the CIEEL spectral maxima are independent of the reaction medium and the means of triggering, whereas the fluorescence spectrum of the authentic CIEEL emitter depends on the solvent. In the aprotic solvents the CIEEL and the fluorescence spectra coincide, while in the protic media the fluorescence maxima of the authentic methyl *m*-oxybenzoate ion are blue-shifted by ca. 50 nm relative to those of the CIEEL emission. Neither exciplex formation nor specific environmental influence of the enzyme on the chemiexcited oxybenzoate accounts for the spectral shift between the CIEEL and the fluorescence emissions. The substitution pattern of the fluorophore is decisive for the observed solvent effects. For the *odd*-substituted methyl oxybenzoate, in which the oxy and the ester functionalities are cross-conjugated, a blue shift applies in the protic media, but not for the *even*-patterned methyl oxynaphthoate, with the oxy and ester groups extendedly conjugated. These divergent spectral observations are rationalized in terms of hydrogen-bonding effects, which are qualitatively substantiated by the semiempirical AM1 calculations.

Introduction

Chemically initiated electron exchange luminescence (CIEEL), a phenomenon of light emission derived from electron-transfer chemistry and originally established by Schuster for the diphenoyl peroxide,¹ constitutes a general chemiluminescent process. The biological prototype of the CIEEL phenomenon¹ constitutes the firefly bioluminescence;² chemical analogues have been documented for α -peroxy lactones³ and appropriate dioxetanes.⁴ The CIEEL-active dioxetanes are of particular interest for numerous commercial applications, most prominently for modern chemiluminescent bioassays.^{5,6} The most successful design^{7,8} of the CIEEL systems developed for the latter purpose utilizes thermally persistent spiroadamantyl-substituted dioxetanes with the protected phenolate ion. The CIEEL of these dioxetanes may be generated at will by treatment with an appropriate reagent (trigger) to release the phenolate ion, which depends on the nature of the protective group. A detailed knowledge on the CIEEL-triggering processes should provide the necessary mechanistic insights for the rational design of more effective CIEEL systems for a broad range of biological, chemical, and medical applications.

Recently we have reported model studies on the phenolate-initiated intramolecular CIEEL process, in which we have examined the reaction kinetics of the silyloxy-substituted spiroadamantyl dioxetanes triggered by fluoride ions⁹ and of the phosphate-protected ones enzymatically triggered by alkaline

phosphatase.¹⁰ The present work on the CIEEL-triggering processes (Scheme 1) is focused on the nature of the excited CIEEL emitter and its dependence on the reaction medium. It was of interest to establish whether the electronically excited CIEEL emitter, namely, the methyl *m*-oxybenzoate ion (*m*-4), is formed as a free species or as an exciplex with the adamantanone (**3**) prior to light emission (Scheme 1). Thus, the chemiluminescence emission might take place from the exciplex (*h* ν') or the free carbonyl fragment (*h* ν). A comparison of the CIEEL spectra with that of the fluorescence for the authentic CIEEL emitter may serve as an experimental diagnostic tool to differentiate these mechanistic alternatives.

Indeed, examples of differences between the chemiluminescence and the fluorescence spectra of the authentic CIEEL emitters have been reported for the intramolecular CIEEL of an amino-substituted dioxetane¹¹ and for the intermolecular CIEEL of the diphenoyl peroxide,¹² which were attributed to the formation of exciplexes. In the former case,¹¹ the polar media promoted exciplex formation, as manifested by the red-shifted CIEEL emission band, while in nonpolar solvents no exciplex was observed. In contrast, although in the intermolecular CIEEL process of the diphenoyl peroxide with triphenylamine¹² also a red shift of the CIEEL spectrum versus the fluorescence emission of the amine was obtained, in solvents with increasing polarity the presumed exciplex emission was reduced.

In view of this solvent dependence, a systematic spectral study of the triggered CIEEL processes for the dioxetanes **1** (Scheme 1) in various protic and aprotic media (H₂O, D₂O, MeOH, MeCN, and DMSO) seemed advisable to assess exciplex involvement. For that purpose, the chemiluminescence spectra of the intramolecularly CIEEL-active intermediate dioxetane phenolate anion **2**, released independently from five dioxetanes **1a–e** (Scheme 1) by different enzymatic and chemical triggers

[†] Dedicated to Professors R. S. H. Lin, D. C. Neckers, J. Saltiel, N. J. Turro, P. J. Wagner, and D. G. Whitten on the occasion of their 60th birthdays.

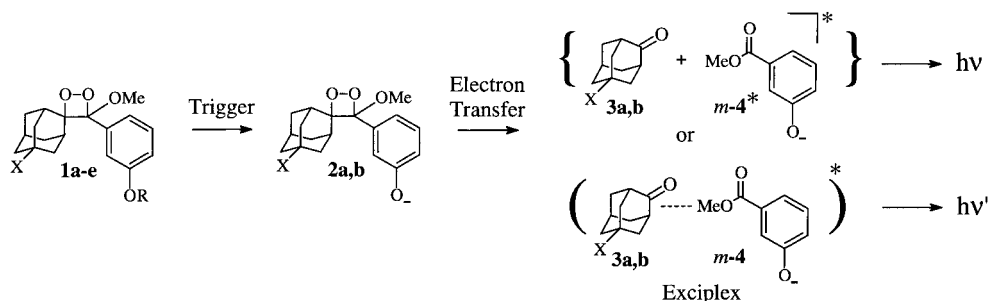
* Corresponding author.

[‡] University of Würzburg.

[§] Tropix, Inc.

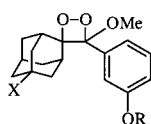
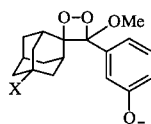
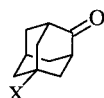
[‡] Russian Academy of Sciences.

SCHEME 1



Dioxetane	X	R	Trigger	Media
1a	H	PO ₃ ²⁻	Alkaline Phosphatase	Aqueous Buffer
1b	Cl	PO ₃ ²⁻	Alkaline Phosphatase	Aqueous Buffer
1c	H	SiMe ₂ tBu	F ⁻	MeCN, DMSO
1d	Cl	SiMe ₂ tBu	F ⁻	MeCN, DMSO
1e	H	H	HO ⁻	H ₂ O, D ₂ O, MeOH

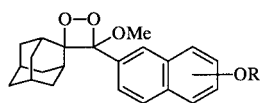
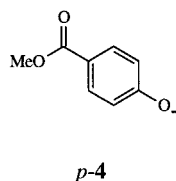
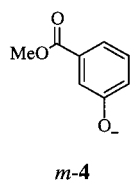
(alkaline phosphatase, HO⁻, and F⁻), were to be examined and compared with the fluorescence spectra of the authentic methyl *m*-oxybenzoate anion (*m*-4) in the same solvents. To test whether the enzyme (alkaline phosphatase) provides specific environmental effects on the excited CIEEL emitter *m*-4 and thereby alters its spectral emission characteristics, the CIEEL spectra of the enzymatically triggered dioxetanes **1a** (AMPPD) and **1b** (CSPD) in the aqueous media were to be measured and compared with the spectra of the base triggering of the hydroxy-substituted dioxetane **1e**, in which no enzyme is involved (Scheme 1).

**1a-e****1a:** X = H, R = PO₃²⁻**1b:** X = Cl, R = PO₃²⁻**1c:** X = H, R = SiMe₂tBu**1d:** X = Cl, R = SiMe₂tBu**1e:** X = H, R = H**2a,b****2a:** X = H, R = PO₃²⁻**2b:** X = Cl, R = PO₃²⁻**3a,b****3a:** X = H**3b:** X = Cl

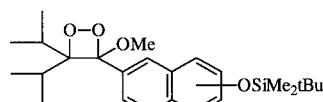
Profound differences in the CIEEL efficiencies have been reported^{6-8,13,14} for a variety of triggered decompositions of dioxetanes, in which regioisomeric phenolate-type emitters are generated. Prominent examples are the *meta*-oxy- and *para*-oxybenzoates *m*-4 and *p*-4 released from the respective dioxetanes **1**^{6-8,13} and the various oxy-substituted naphthoates **7** from the dioxetanes **5**^{7d,8b} and **6**.¹⁴ To understand these differences, a qualitative pictorial rationalization has been forwarded for the regioisomeric oxybenzoates **4**,¹³ and semiempirical MO calculations have been applied to the oxynaphthoates **7**.^{7b} In the latter study, the regioisomeric fluorophores were classified in terms of *odd* emitters [e.g. *m*-4 or **7**(2,5)], in which the oxy and ester functionalities are cross-conjugated, and *even* emitters [e.g. *p*-4 or **7**(2,6)] with extendedly conjugated groups. Since the phenolate-type ions (oxyanions) are sensitive to solvatochromic effects,^{15,16} in both the absorption and emission properties, it was advisable to examine such solvent effects on the regioisomeric oxybenzoates *m,p*-4. As model systems also the naphtholate regioisomers α,β -**8** were chosen since, for these, detailed work on the spectral solvent effects exists.¹⁵⁻¹⁷ Presently we report our results on these spectral studies and show that semiempirical calculations (AM1) are quite helpful to rationalize the observed trends in terms of the *odd-even* classification of the emitters generated in the triggered decomposition of the dioxetanes.

Experimental Section

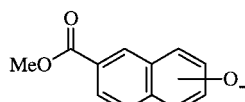
Materials. The dioxetanes AMPPD {disodium 3-(2'-spiroadamantane)-4-methoxy-4-(3''-phosphoryloxy)phenyl-1,2-dioxetane} (**1a**) and CSPD {disodium 3-(2'-spiro-5'-chloroadamantane)-4-methoxy-4-(3''-phosphoryloxy)phenyl-1,2-dioxetane} (**1b**) as well as sodium 3-(adamantylidene-methoxy-methyl)phenolate were made available by Tropix, Inc. (Bedford, MA) and used without further purification. The dioxetanes 3-(2'-spiroadamantane)-4-methoxy-4-(3''-butyldimethylsilyloxy)phenyl-1,2-dioxetane (**1c**) and 3-(2'-spiro-5'-chloroadamantane)-4-methoxy-4-(3''-butyldimethylsilyloxy)phenyl-1,2-dioxetane (**1d**), methyl 3-silyloxybenzoate, and sodium methyl 3-oxybenzoate were kindly made available by Dr. M. Schulz.¹⁸



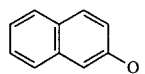
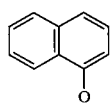
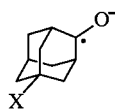
5a,b
5a: R = Ac
5b: R = PO₃²⁻



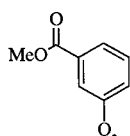
6



7

 β -8 α -8

9a,b
9a: X = H
9b: X = Cl



10

Methyl *meta*- and *para*-hydroxybenzoates, α - and β -naphthols and the solvents acetonitrile, dimethyl sulfoxide (DMSO), and methanol (UV-spectral grade) were obtained from Fluka. As fluoride ion source, a 1 M stock solution of tetrabutylammonium fluoride in tetrahydrofuran (THF) [Aldrich] was used. The alkaline phosphatase (Biozyme ALPI 12G) was obtained from Biozyme (U.K.).

Methoxy(3-hydroxyphenyl)methyleneadamantane¹⁹ was prepared by hydrolysis of 788 mg (2.69 mmol) of sodium 3-(adamantylidene-methoxymethyl)phenolate, suspended in 10 mL of ethyl acetate, with 3.50 g of ammonium chloride in 12 mL of water cooled by means of an ice bath. The aqueous layer was separated and extracted with 5 mL of ethyl acetate. The organic extract was washed with water (5 mL) and dried (Na₂SO₄), the solvent was removed by distillation (40 °C/20 Torr), and the oily residue was triturated with 5 mL of hexane. Upon removal of the solvent (20 °C/20 Torr), 660 mg (91%) of a colorless solid was obtained; its spectral data match those reported.¹⁹

3-(2'-Spiroadamantane)-4-methoxy-4-(3''-hydroxy)phenyl-1,2-dioxetane (1e).¹⁹ A sample of 500 mg (1.85 mmol) of methoxy(3-hydroxyphenyl)methyleneadamantane was dissolved in 5 mL of methylene chloride, ca. 10 μ g of tetraphenylporphine was added, and the solution was cooled by means of an ethanol bath to -10 °C. The solution was irradiated for 30 min by two sodium lamps (Philips G/98/2-SON, 150 W) while passing a gentle stream of oxygen gas, which was dried over CaCl₂/

silica gel/P₂O₅. The solvent was removed (ca. 20 °C and 20 Torr) and the residue (550 mg) was chromatographed on silica gel (50 g) with methylene chloride as eluent to yield 320 mg (57%) of a pale yellow oil; its spectral data match those reported.¹⁹

Spectral Measurements. The fluorescence and the chemiluminescence (CIEEL) spectra were recorded on a Perkin-Elmer LS 50 luminescence spectrophotometer. Absorption spectra were measured on a Hitachi U-3200 spectrophotometer. For the comparison of the fluorescence and the chemiluminescence spectra with different intensities, these spectra were normalized by adjusting the maximum intensities to the same value. This procedure was done with the normalization option as implemented in the Perkin-Elmer Fluorescence Data Manager (FLDM) set of programs. The fluorescence quantum yields were measured by the conventional procedure¹⁶ versus quinine bisulfate ([QBS] = 1.19 \times 10⁻⁶ M) in 1 N H₂SO₄ as the fluorescence standard ($\Phi_{\text{QBS}}^{\text{fl}}$ = 0.55).²⁰ The sodium or potassium methyl *m,p*-oxybenzoate (*m,p*-4) and α,β -naphtholate (α,β -8) anions in the protic solvents (H₂O, D₂O, and MeOH) were prepared by the reaction of the neutral forms with an excess of sodium or potassium hydroxide. In the aprotic solvents (MeCN and DMSO), solutions of the oxyanions 4 and 8 were prepared by addition of small (0.05–0.08% of volume) portions of their stock solutions in 1 N aqueous NaOH and KOH. Solutions of the tetrabutylammonium oxybenzoate ion *m*-4 in MeCN and DMSO were prepared by the reaction of the methyl 3-silyloxybenzoate with an excess of fluoride ions in these solvents ([*n*-Bu₄NF] = 7.67 \times 10⁻⁴ M). As control measurements, the fluorescence spectra of the oxybenzoate ion *m*-4 were measured on the reaction mixtures obtained from the dioxetanes 1 after their total triggered decomposition under the appropriate conditions (cf. the legend for Figure 1). The pH values were determined by means of a pH electrode (Hamilton Bonaduz AG).

Computational Methods. The semiempirical calculations are based on the AM1 method²¹ as implemented in the VAMP 5.0²² software package and run on a Silicon Graphics Indigo workstation. The bulk-polarity effects for each solvent were determined by the self-consistent-reaction-field (SCRFF)²³ option as provided in the VAMP 5.0 set of programs. With this SCRFF approach, the anions were calculated within an evacuated cavity that is surrounded by a polarizable continuum; the latter simulates the bulk solvent. The excited-state calculations were performed by using the singles-plus-pair-excitation configuration interaction (PECI)²³ approach with an active space of 10 molecular orbitals (MOs).

Results

Spectral Data. The CIEEL spectra of the dioxetanes 1a,b,e and the fluorescence spectra of the methyl *m*-oxybenzoate ion (*m*-4), the common fluorophore generated from the dioxetanes 1 on triggering, in protic (H₂O, D₂O, and MeOH) and aprotic (MeCN and DMSO) solvents are exhibited in Figure 1. It is noteworthy that the CIEEL spectra of all five dioxetanes 1a–e possess the same emission maxima ($\lambda_{\text{max}}^{\text{CIEEL}}$ = 465–466 nm) in all protic and aprotic media. In contrast, the fluorescence spectra of the methyl *m*-oxybenzoate ion (*m*-4) are blue-shifted ($\Delta\lambda_{\text{max}}^{\text{fl}}$ = 51 nm) in the protic solvents versus the aprotic ones. No difference was observed in the CIEEL spectra of the chlorinated (1b,d) versus unchlorinated (1a,c) dioxetanes (Figure 1). The CIEEL spectra of the enzymatically triggered dioxetanes 1a,b in the aqueous media match well those of the base

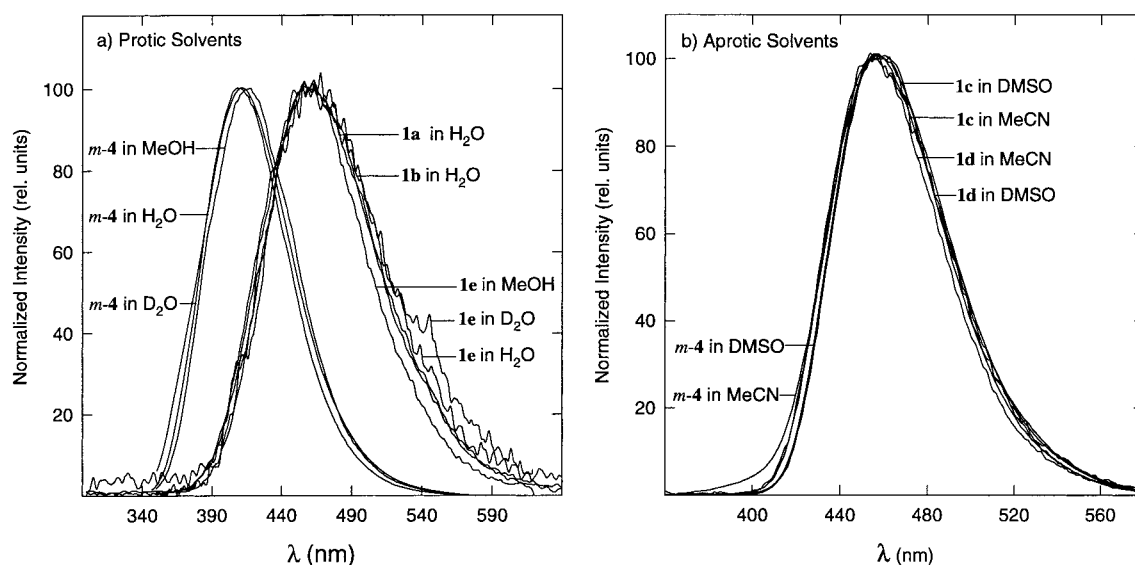
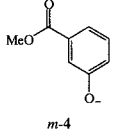
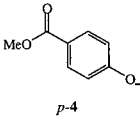
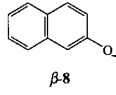
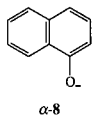


Figure 1. Normalized CIEEL and fluorescence spectra in the protic (a) and aprotic (b) media. (a) CIEEL emissions (at the right) in the alkaline-phosphatase-triggered ([alkaline phosphatase] = 2×10^{-7} M) decomposition of the dioxetanes **1a** (1.7×10^{-3} M) and **1b** (2.7×10^{-3} M) in 0.05 M carbonate buffer, 1 mM MgCl_2 at pH 9.5 and room temperature (ca. 20 °C), and that of the NaOH-triggered (pH 12.7) hydroxy-substituted dioxetane **1e** (3.4×10^{-3} M) in H_2O , D_2O , and MeOH, and the fluorescence emission (at the left, $\lambda_{\text{ex}} = 337$ nm) of the authentic methyl *m*-oxybenzoate ion (*m-4*) = 5×10^{-5} M under the latter conditions. (b) CIEEL emissions in the fluoride-ion-triggered decomposition ($[\text{n-Bu}_4\text{NF}] = 7.67 \times 10^{-4}$ M) of the dioxetanes **1c,d** (10^{-4} M) at room temperature in MeCN and DMSO and the fluorescence emission ($\lambda_{\text{ex}} = 337$ nm) of the methyl *m*-oxybenzoate (*m-4*) = 10^{-5} M under the same conditions.

TABLE 1: CIEEL ($\lambda_{\text{max}}^{\text{CIEEL}}$), Fluorescence ($\lambda_{\text{max}}^{\text{fl}}$), and Absorption ($\lambda_{\text{max}}^{\text{abs}}$) Maxima^a and the Experimentally Observed Shifts of the Fluorescence ($\Delta\lambda_{\text{max}}^{\text{fl}}$) and the Absorption ($\Delta\lambda_{\text{max}}^{\text{abs}}$) Maxima for the Oxyanions **4 and **8** in Water Relative to Other Solvents, the Calculated Contribution of the Solvent Bulk Polarity ($\Delta\lambda^{\text{bulk}}$),^b and the Fluorescence Quantum Yields (Φ^{fl})^{a,c}**

	1	2	3	4	5	6	7	8	9	10
anion	type	solvent	$\lambda_{\text{max}}^{\text{CIEEL}}$ (nm)	$\lambda_{\text{max}}^{\text{fl}}$ (nm)	$\Delta\lambda_{\text{max}}^{\text{fl}}$ (nm)	$\lambda_{\text{max}}^{\text{abs}}$ (nm)	$\Delta\lambda_{\text{max}}^{\text{abs}}$ (nm)	$\Delta\lambda^{\text{bulk}}$ (nm)	Φ^{fl} d,e	
 <i>m-4</i>	I	D_2O	466	415	-	316	-	-		
		H_2O	466 [ca. 470 ^g]	415	-	316	-	-	0.28 ± 0.04	
		MeOH	465	415	-	316	-	1	0.27 ± 0.06	
		MeCN	466	466	51	366	50	8	0.29 ± 0.05^f [0.21 ^h]	
		DMSO	466 [470 ^h , 463 ⁱ]	466 [470 ^h]	51	388	72	9	0.50 ± 0.05^f [0.44 ^h]	
 <i>p-4</i>	II	H_2O		344	-	297	-	-	$(0.6 \pm 0.25) \times 10^{-3}$	
		MeOH		345	1	297	-	-	$(2.1 \pm 0.5) \times 10^{-3}$	
		MeCN		349	5	313	16	3	$(2.9 \pm 0.6) \times 10^{-3}$	
		DMSO		352	8	326	29	3	$(3.6 \pm 0.6) \times 10^{-3}$	
 β -8	I	H_2O		419 [420 ^j]	-	345 [347 ^l]	-	-	0.31 ± 0.04 [0.36 ^l]	
		MeOH		420 [420 ^j]	-	348 [349 ^l]	3 [2 ^l]	-	0.26 ± 0.03 [0.23 ^l]	
		MeCN		450 [451 ^l]	31 [31 ^l]	379 [380 ^l]	34 [33 ^l]	10	0.47 ± 0.04	
		DMSO		454 [456 ^l]	35 [36 ^l]	394 [396 ^l]	49 [49 ^l]	10	0.79 ± 0.05 [0.93 ^l]	
 α -8	II	H_2O		464 [462 ^l , 465 ^m]	-	334 [335 ^l]	-	-	0.10 ± 0.02 [0.12 ⁿ , 0.114 ^o]	
		MeOH		464 [464 ^l]	-	334 [334 ^l]	-	-	0.09 ± 0.01	
		MeCN		472	8	347	13	7	0.14 ± 0.03	
		DMSO		473	9	357	23	8	0.25 ± 0.05	

^a Literature data are shown in brackets. ^b Calculated by the AM1 method with the SCRF option, which is provided in the VAMP 5.0 set of programs. ^c Measured versus quinone bisulfate as the fluorescence standard ([QBS] = 1.19×10^{-6} M) in 1 N H_2SO_4 . ^d Each value is an average of at least four measurements. ^e KOH was used as base (pH 11.5). ^f $[\text{n-Bu}_4\text{NF}] = 5.1 \times 10^{-4}$ M. ^g Ref 7c. ^h Ref 8a. ⁱ Ref 14. ^j Ref 16. ^k Ref 17. ^l Ref 25. ^m Ref 26. ⁿ Ref 27. ^o Ref 28.

triggering of the hydroxy-substituted dioxetane **1e**, in which no enzyme is involved (Figure 1a).

The experimental data on the CIEEL ($\lambda_{\text{max}}^{\text{CIEEL}}$), the fluorescence ($\lambda_{\text{max}}^{\text{fl}}$) and the absorption ($\lambda_{\text{max}}^{\text{abs}}$) maxima for the

oxyanions **4** and **8** in the various solvents are given in Table 1 (columns 4, 5, and 7). From these the shifts of the fluorescence ($\Delta\lambda_{\text{max}}^{\text{fl}}$) and the absorption ($\Delta\lambda_{\text{max}}^{\text{abs}}$) maxima in the various solvents relative to water are summarized in Table 1 (columns

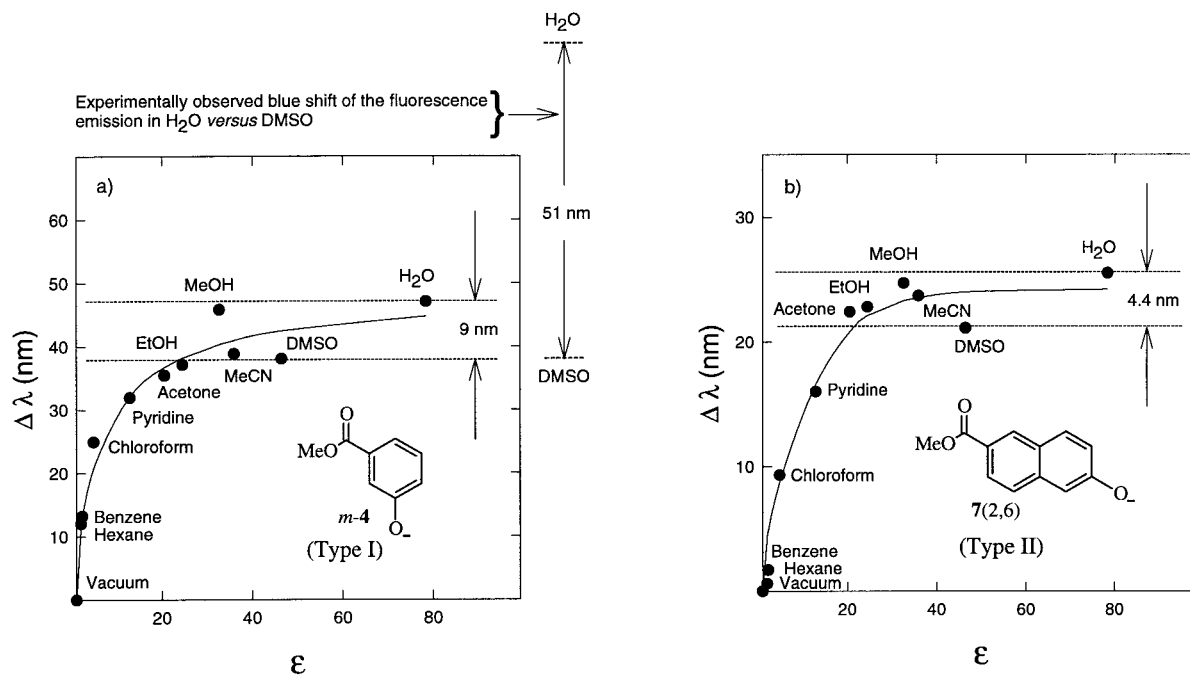


Figure 2. Calculated (AM1 method, for details cf. Experimental Section) contribution of the solvent bulk-polarity effect to the hypsochromic shift of the optical S_0-S_1 (0-0) transition in the CIEEL emitters: (a) type-I methyl *m*-oxybenzoate ion (*m*-4) and (b) type-II methyl 6-oxy-2-naphthoate ion [7(2,6)] in the different media relative to vacuum plotted versus the dielectric constant ϵ . For comparison, the experimentally observed blue shift (51 nm) of the fluorescence of *m*-4 in water relative to DMSO is shown.

6 and 8), together with the respective fluorescence yields (Φ^{fl}) in these solvents (column 10). For comparison, the relevant literature data are also shown in Table 1.

Contrary to the methyl *m*-oxybenzoate ion (*m*-4), the blue shifts of the fluorescence spectra of the *para* regioisomer *p*-4 are quite small in the protic versus the aprotic media (Table 1, column 6). Thus, *meta* substitution leads to a significantly larger hypsochromic effect on the fluorescence emission than the *para* one. A similar trend is apparent for the two naphtholate anion regioisomers α,β -8 (Table 1, column 6). Whereas the fluorescence emission of the β -naphtholate ion (β -8) is strongly blue-shifted in the protic versus the aprotic solvents, the hypsochromic shift for α -naphtholate ion (α -8) is much smaller. Thus, on the basis of these trends in the $\Delta\lambda_{\text{max}}^{\text{fl}}$ values, the oxyanions may be classified as type I, which possess a strong blue shift of the fluorescence in the protic media versus the aprotic ones, e.g. the methyl *m*-oxybenzoate (*m*-4) and β -naphtholate (β -8) anions, and type II, whose fluorescence is only slightly dependent on the solvent, namely the methyl *p*-oxybenzoate (*p*-4) and the α -naphtholate (α -8) ions. Consequently, the methyl 6-oxy-2-naphthoate anion [7(2,6)], the authentic chemiluminescence emitter in the CIEEL triggering of the dioxetanes 5(2,6) and 6(2,6), belongs to the type-II category since, as it was established before,^{8b,14} its fluorescence spectral maximum is the same in H_2O ^{8b} and DMSO.¹⁴ The shifts ($\Delta\lambda_{\text{max}}^{\text{abs}}$) of the absorption maxima in the various solvents relative to water are also smaller for the type-II versus the type-I regioisomers (Table 1, column 8).

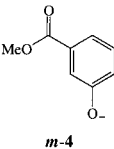
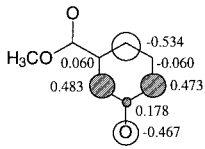
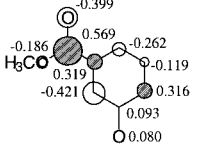
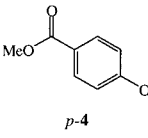
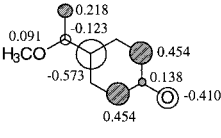
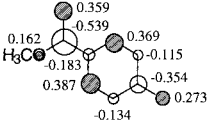
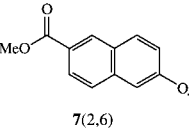
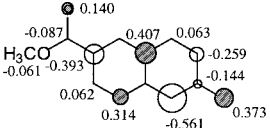
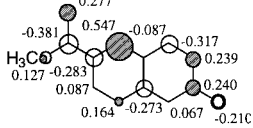
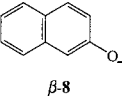
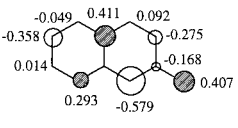
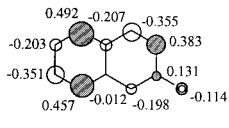
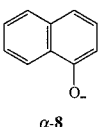
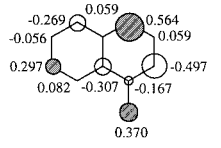
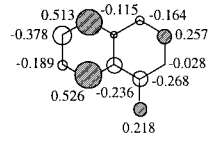
The fluorescence quantum yields (Table 1, column 10) characterize the oxyanions *m*-4 and α,β -8 as good fluorophores in all protic and aprotic solvents used herein. However, a dramatic (ca. 100 times) reduction of the fluorescence yield was observed for the *para* isomer of the methyl oxybenzoate ion (*p*-4).

Computational Results. Computer simulation of the bulk electrostatic properties of the various solvents has revealed hypsochromic shifts in the S_0-S_1 transitions for all the

oxyanions 4, 7, and 8 in these media relative to vacuum. This is exemplarily illustrated in Figure 2 for the CIEEL emitters oxybenzoate ion *m*-4 (type I) and oxynaphthoate ion [7(2,6)] (type II). As one can see from Figure 2, the computed bulk-polarity effects, represented by the hypsochromic shifts of the S_0-S_1 (0-0) transition of the oxyanions, are quite similar in all polar solvents of interest for the present study (DMSO, MeCN, MeOH, and H_2O). For example, the difference ($\Delta\lambda^{\text{bulk}}$) in the computed bulk-polarity effects between DMSO and H_2O constitutes 9 nm (experimentally, $\Delta\lambda_{\text{max}}^{\text{fl}} = 51$ nm) for the type-I oxybenzoate ion (Figure 2a) and only 4.4 nm (experimentally^{8b,14}, $\Delta\lambda_{\text{max}}^{\text{fl}} = 0$ nm) for the type-II oxynaphthoate anion (Figure 2b). Similar trends apply to the remaining oxyanions (Table 1, column 9). Thus, the computed $\Delta\lambda^{\text{bulk}}$ values (Table 1, column 9) are comparable to the experimentally observed solvatochromic shifts ($\Delta\lambda_{\text{max}}^{\text{fl}}$) of the fluorescence emission only for the type-II anions and are much smaller than the experimental $\Delta\lambda_{\text{max}}^{\text{fl}}$ values for the type-I oxyanions (Table 1, column 6). Consequently, the contribution of the bulk polarity ($\Delta\lambda^{\text{bulk}}$) to the total hypsochromic shift ($\Delta\lambda_{\text{max}}^{\text{fl}}$) of the fluorescence emission of the type-I anions in the protic versus the aprotic media does not account for the observed experimental results.

The calculated HOMO and LUMO (π type) data for the oxyanions *m,p*-4, 7(2,6), and α,β -8 are collected in Table 2 (columns 3 and 4). In these orbital pictures, the carbon framework of the conjugated system is contained in the plane of the paper (*x,y* coordinates) and the π orbitals are oriented along the *z* axis. The calculated total and π charges (q) on the phenolate oxygen atom of the oxyanions 4, 7, and 8 in the ground (S_0) and in the first singlet-excited (S_1) states and the differential charges (Δq) for the $S_0 \rightarrow S_1$ excitation are given in columns 6-8 of Table 2. Noteworthy is the fact that the total and the π differential charges (Δq) coincide for all oxyanions of interest (column 8). More significant for our subsequent discussion, the difference in the HOMO and the LUMO coefficients (columns 3 and 4) and the differential charges (column 8) centered on the phenolate oxygen atom

TABLE 2: HOMO and LUMO Coefficients, the Total and the π Charges on the Phenolate Oxygen Atom of the Oxyanions 4, 7, 8 in the Ground (S_0) and in the First Singlet-Excited (S_1) States, and the Differential Charge (Δq) for the $S_0 \rightarrow S_1$ Excitation

1	2	3	4	5	6	7	8
anion	type	HOMO ^a	LUMO ^a	charge (q)	$q(S_0)$	$q(S_1)$	Δq^b
	I			total π	0.52 0.44	0.32 0.22	0.20 0.22
	II			total π	0.48 0.34	0.37 0.24	0.11 0.10
	II			total π	0.46 0.28	0.36 0.18	0.10 0.10
	I			total π	0.50 0.33	0.35 0.18	0.15 0.15
	II			total π	0.49 0.27	0.39 0.18	0.10 0.09

^a Calculated by the AM1 method as implemented in VAMP 5.0 software package. ^b $\Delta q = q(S_0) - q(S_1)$.

(Table 2) are markedly larger for the type-I oxybenzoate (*m*-4) and naphtholate (β -8) ions, whose fluorescence is strongly blue-shifted in the protic versus the aprotic media (Table 1, columns 5 and 6).

Mechanistic Discussion

The comparative chemiluminescence and fluorescence spectral studies presented herein reveal the intriguing fact that the CIEEL spectral maxima in all triggered processes of Scheme 1 are independent of the reaction medium (Figure 1; Table 1, column 4), whereas the fluorescence spectrum of the authentic CIEEL emitter, namely, the methyl *m*-oxybenzoate anion (*m*-4), depends on the solvent (Figure 1; Table 1, column 7). In the aprotic solvents MeCN and DMSO the CIEEL and the fluorescence spectra coincide (Figure 1b), while in the protic media H₂O, D₂O, and MeOH the fluorescence maxima of the authentic methyl *m*-oxybenzoate ion (*m*-4) are blue-shifted by ca. 50 nm relative to those of the CIEEL emission (Figure 1a; Table 1, columns 4 and 5). In contrast, the CIEEL spectra of the enzymatically triggered naphthoate-substituted dioxetanes **5**(2,6) in aqueous media^{7d,8b} and the fluorescence spectrum of the authentic naphthoate **7**(2,6) in water^{8d} were reported to match well. To rationalize these diverging spectral observations, the present experimental and computational data shall be now mechanistically scrutinized.

The coincidence of the CIEEL spectra of the alkaline-phosphatase-triggered dioxetanes **1a** and **1b** with the spectrum

of the base-triggered hydroxy-substituted dioxetane **1e** in the aqueous media (Figure 1a) speaks against the possibility that any specific enzyme environmental effects are involved in the generation of the chemically excited methyl *m*-oxybenzoate ion (*m*-4*). Even if the dioxetane were to decompose within the enzyme, the observed spectral shifts cannot be explained in terms of substrate–enzyme associations. Since we have previously found¹⁰ that the intermediate phenolate ion **2**, which is formed in the enzymatic dephosphorylation of the dioxetanes **1a,b** (Scheme 1), is a relatively long-lived species (lifetime of ca. 1 min in water at 37 °C), most probably it leaves the enzyme pocket *before* its cleavage to the chemically excited oxybenzoate *m*-4*, and no enzyme environmental influence should become discernible.

The observed spectral shifts (Figure 1a) can also not be attributed to the formation of an exciplex between the *m*-4* and **3** ketone products (Scheme 1) in the triggered decomposition of dioxetane **1**, as suggested by the solvent effects in Table 1. Polar solvents generally enhance exciplex formation;²⁴ however, for the present case, in MeOH ($\epsilon = 32.7$) and H₂O ($\epsilon = 78.4$) spectral shifts (Figure 1) are evident, but not in MeCN ($\epsilon = 35.9$) and DMSO ($\epsilon = 46.5$). Thus, the observed difference between the CIEEL and the fluorescence spectra for the oxybenzoate ion *m*-4 does not correlate with the solvent polarity, but rather depends on whether the solvent is protic or not.

Contrary to the behavior of the *odd*-substituted group in the dioxetanes **1**, for the *even*-substituted ones **5**(2,6) no spectral

shift of the chemiluminescence relative to the fluorescence of the authentic CIEEL emitter **7**(2,6) was observed;^{8b} consequently, the structure of the fluorophore plays also a significant role in this phenomenon. To understand this feature, the elucidation of the solvatochromic effects on the oxyanions with various substitution patterns is instructive. The fluorescence and the absorption spectra of the oxyanion *m*-**4** are strongly blue-shifted in the protic versus the aprotic solvents (Table 1, columns 6 and 8). That bulk polarity is not responsible for the observed solvatochromic shifts is confirmed by the calculated contributions $\Delta\lambda^{\text{bulk}}$ for the oxyanion *m*-**4** in the various solvents relative to water (Table 1, columns 9). They are much smaller than the experimental $\Delta\lambda_{\text{max}}^{\text{fl}}$ and $\Delta\lambda_{\text{max}}^{\text{abs}}$ values (Table 1, columns 6 and 8), which is illustrated in Figure 2a. Thus, instead of mere bulk polarity, it is the protic nature of the solvent that is important in promoting the observed spectral shifts, which suggest hydrogen bonding as the mechanism of action for the oxybenzoate anion *m*-**4**. Contrary to the latter, for the oxynaphthoate anion **7**(2,6) such a blue shift is not found in aqueous media^{8b} versus DMSO;¹⁴ clearly, the hydrogen-bonding effects on the spectra of the oxyanions are strongly dependent on their structure. In fact, in the Results section we have classified the oxyanions as type I (strongly blue-shifted) and type II (moderately blue-shifted) in protic solvents, so that *m*-**4** belongs to the former and **7**(2,6) to the latter categories. A similar trend is noticed for the β -**8** (type-I) and α -**8** (type-II) naphtholate ions (Table 1, columns 6 and 8), while the *para*-oxybenzoate *p*-**4** is a type-II anion.

The spectral data (Table 1, columns 6 and 8) clearly establish that hydrogen-bonding effects are responsible for the blue shifts in the protic versus the aprotic solvents, but the fundamental question remains why the type-I and the type-II anions behave so differently. To rationalize qualitatively this difference, the results of the semiempirical AM1 calculations in Table 2 are relevant. The configuration-interaction calculations on the oxyanions **4**, **7**(2,6), and **8** reveal for all that the HOMOs and LUMOs are of the π type (Table 2, columns 3 and 4). Most significantly, the difference in the HOMO and the LUMO coefficients on the phenolate oxygen atom is markedly larger for the type-I oxyanions *m*-**4** and β -**8** than for the type-II ones **4**, **7**(2,6), and **8**. For all oxyanions, the large HOMO coefficients on the phenolate oxygen atom guarantee appreciable hydrogen bonding at this site in the ground state. In contrast, the hydrogen bonding should be markedly weaker in the excited state for the type-I anions *m*-**4** and β -**8** due to the small LUMO coefficients on the phenolate oxygen atom (Table 2, column 4). Consequently, this simple HOMO/LUMO analysis suggests that the ground and the singlet-excited states are stabilized by hydrogen bonding to different degrees for the type-I and type-II oxyanions. In fact, the differential total and π charges (Δq) between the first singlet-excited (S_1) and ground (S_0) states also reflect this trend (Table 2, column 8). Thus, for the type-I ions the Δq values are substantially larger (about twice) than for the type-II ones, which confirms that the differences in hydrogen bonding in the ground and the first singlet-excited states are more pronounced for the type-I oxyanions. The hydrogen-bonding effects are graphically presented in Figure 3 for the photo- and chemiexcited type-I and type-II anions in protic versus aprotic solvents.

For the type-I oxyanions *m*-**4** and β -**8** (Figure 3a), the greater charge (significantly larger HOMO compared to LUMO coefficients) at the phenolate oxygen atom stabilizes the relaxed ground state (S_0) more effectively through hydrogen bonding in the protic solvents than the first singlet-excited state (S_1).

This accounts for the strong blue shifts ($\Delta\lambda_{\text{max}}^{\text{abs}}$ and $\Delta\lambda_{\text{max}}^{\text{fl}}$) for the absorption ($S_0 + hv \rightarrow S_1^{\text{FC}}$) and the fluorescence processes ($S_1 \rightarrow S_0^{\text{FC}} + hv$) in protic versus aprotic solvents (Table 1, columns 6 and 8). Contrary to the type-I anion, the more similar charges (and HOMO/LUMO coefficients) in the ground (S_0) and the first singlet-excited (S_1) states in the case of the type-II oxyanions *p*-**4**, **7**(2,6), and α -**8** (Figure 3b) provide no significant differential stabilization through hydrogen bonding. For these oxyanions, much smaller spectral changes are expected in the protic versus aprotic solvents, again as verified by the experimental data (Table 1, columns 6 and 8). Thus, the more pronounced reduction of the electron density at the phenolate oxygen atom during these π excitations for the type-I versus type-II oxyanions qualitatively accounts for the observed solvatochromic shifts.

This phenomenon seems to be general for the oxybenzoate **4** and oxynaphthoate **7** regioisomers and forms the basis of classifying emitters and their corresponding dioxetane precursors as *odd* (type-I) and *even* (type-II) species in regard to whether they are cross-conjugated or extendedly conjugated.^{7b} Indeed, a considerably larger reduction of the electron density at the oxy functionality on excitation has been reported for the *odd*- versus the *even*-patterned oxynaphthoate regioisomers **7**.^{7b} The AM1 semiempirical calculations performed in this work on the *meta*- and the *para*-regioisomeric oxybenzoates **4** confirm that these species follow the same trend.

The contrasting absorption and fluorescence spectral properties of type-I versus type-II phenolate ions are nicely accounted for in terms of the differences in the relative stabilization of the ground and first singlet-excited states due to hydrogen bonding, a consequence of differential charge distribution or HOMO/LUMO coefficients at the oxyanion site. These spectral features alone, however, do not explain the differences in the chemi- versus photoexcited emissions (Figure 1; Table 1, columns 4 and 5). The facts are that for type-I *m*-oxybenzoate, the triggered CIEEL emission from dioxetane **1** is ca. 50 nm red-shifted in protic solvents versus direct photoexcitation of this oxyanion, while in aprotic solvents these emission are identical within the experimental error. These spectral data should be compared to the type-II *p*-oxybenzoate *p*-**4**, but its fluorescence emission is so low (Table 1, column 10) that it was difficult to measure the spectra of the triggered CIEEL emissions from the respective dioxetane. For this reason, we take the type-II oxyanion **7**(2,6) as comparison, for which it has been reported that its chemi- and photoexcited species emit at the same wavelength irrespective of whether protic (H_2O^{8b}) or aprotic (DMSO¹⁴) solvents are used.

To rationalize these spectral differences between the type-I and type-II oxyanions, it is essential to consider the mechanism of the CIEEL process of the dioxetane oxyanion **2** (Scheme 2). A solvent-caged radical pair is produced on electron transfer (ET) and subsequent dioxetane cleavage, which on electron back-transfer (BET) affords the chemiexcited *m*-oxybenzoate ion *m*-**4*** from the dioxetane anion **2a**. The point is that the oxyl-benzoate radical **10** intervenes as immediate precursor to the singlet-excited *m*-**4*** oxyanion, the former a species with negligible hydrogen bonding compared to the ground-state oxyanion *m*-**4**. In fact, as the computational data (Table 2) have revealed, for this type-I oxyanion the charge (q) at the phenolate oxygen atom is low in the S_1 state (small LUMO versus HOMO coefficients). Consequently, during the CIEEL process, apparently the Franck-Condon ground state is negligibly stabilized through hydrogen bonding, and hence, a red-shifted emission ($h\nu^{\text{CIEEL}}$) is observed compared to photoexcitation (Figure 3a).

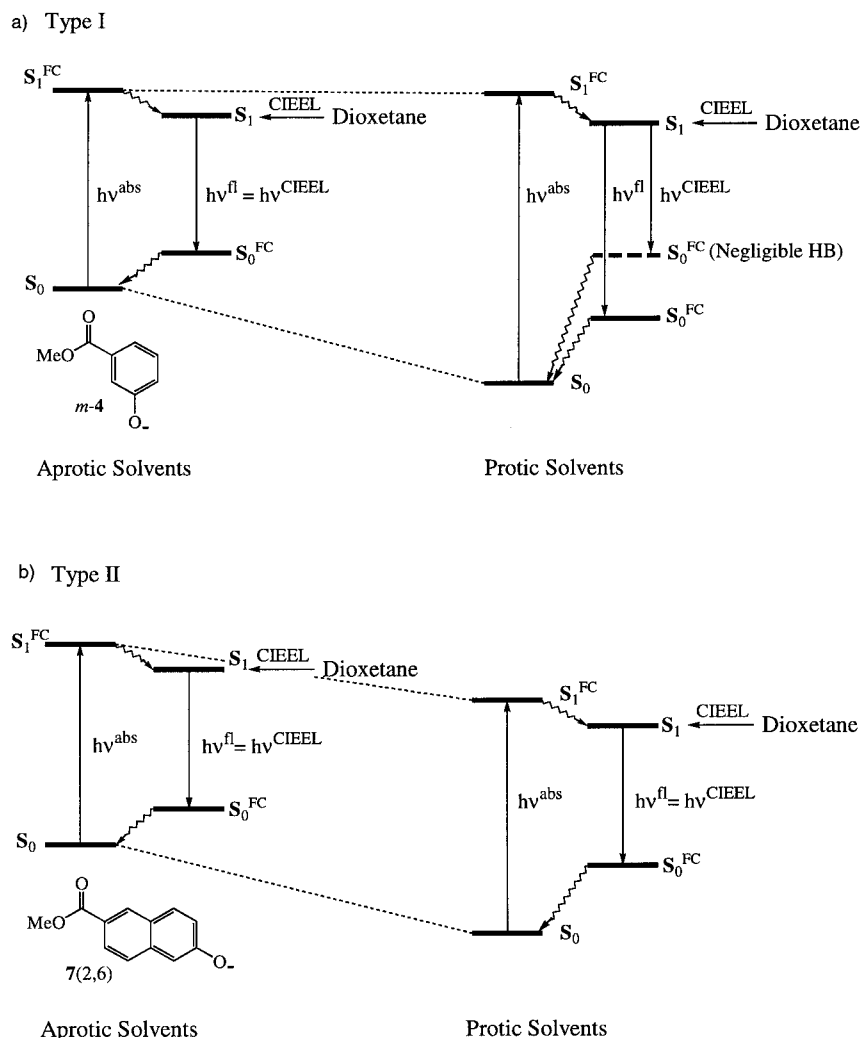
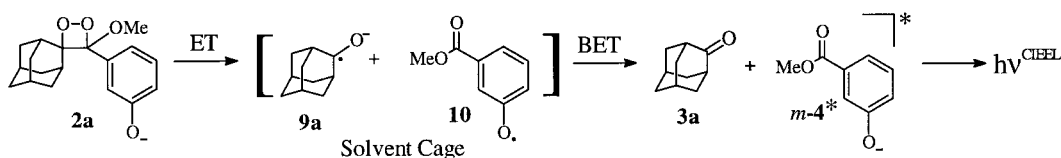


Figure 3. Schematic representation of the hydrogen-bonding effects on the photo- and chemiexcited type-I (a) and type-II (b) oxyanions in the protic versus aprotic solvents; FC refers to the Franck–Condon states, HB to hydrogen bonding, $h\nu^{\text{abs}}$ to absorption, $h\nu^{\text{fl}}$ to fluorescence, and $h\nu^{\text{CIEEL}}$ to chemiluminescence.

SCHEME 2



Moreover, since both the chemiexcited singlet (S_1) and the Franck–Condon ground (S_0^{FC}) states are negligibly stabilized by the hydrogen bonding in the protic media (Figure 3a), no spectral difference between the CIEEL emissions ($S_1 \rightarrow S_0^{\text{FC}} + h\nu^{\text{CIEEL}}$) is observed in the protic and the aprotic solvents (Table 1, column 4). For the photoexcited process, as already discussed, despite the lower charge (q) at the phenolate oxygen atom, enough protic solvent molecules are still associated with the singlet-excited state S_1 (weak hydrogen bonding). Thus, during the fluorescence emission ($h\nu^{\text{fl}}$) of the photoexcited species, in contrast to the chemiexcited $m\text{-}4^*$ of the CIEEL case, the Franck–Condon ground state, stabilized by hydrogen bonding, is reached. Such a “memory effect” in the photoexcitation process has been suggested for the naphtholate anion $\beta\text{-}8^{16}$ to account for the fluorescence spectral shifts in the contact ion pairs. To attribute the observed solvatochromic effects to exciplex formation in the chemiexcitation process is difficult to accept because why should it only operate in protic but not

in nonprotic media for the type-I and not at all in the type-II oxyanion?

For a type-II oxyanion such as 7(2,6), in contrast, our graphical presentation in Figure 3b displays insignificant spectral differences between chemi- and photoexcitation. Like for the type-I case, again the oxyl radical in the chemiexcitation process (Scheme 2) also provides little opportunity to associate protic molecules with the type-II 7(2,6) oxyanion through hydrogen bonding; however, unlike the type-I case, the LUMO coefficients at the phenolate oxygen atom in the type-II oxyanions are relatively large and more similar to their HOMO coefficients such that similar stabilization by hydrogen bonding operates both in the S_1 and S_0 states and no significant solvatochromic effect is expected. Consequently, the chemiluminescence emission ($h\nu^{\text{CIEEL}}$) of such type-II oxyanions matches that of the fluorescence ($h\nu^{\text{fl}}$) in protic as well as aprotic solvents, as is found experimentally.^{8b} Also the more similar charges at the phenolate oxygen atoms for the singlet-excited (S_1) and

ground (S_0) states of the type-II oxyanions substantiate this trend.

The present spectral study discloses that the substitution pattern of the emitters generated in the triggered decomposition of the CIEEL-active dioxetanes is of prime importance for the observed solvatochromic effects. Whereas for the *even* substitution no significant differences in the hydrogen bonding of the chemi- and photoexcited CIEEL emitter is found, the *odd* substitution displays a significant blue shift of the fluorescence versus the chemiluminescence spectra in the protic media.

Acknowledgment. Generous funding by the Deutsche Forschungsgemeinschaft (Sonderforschungsbereich 172 "Molekulare Mechanismen kanzerogener Primärveränderungen") is gratefully appreciated. A.V.T. thanks the Deutsche Forschungsgemeinschaft for a visiting grant (April–July 1997) and the Rossiiskii Fond Fundamental'nykh Issledovani (Grant No. 96-03-34142) for financial support. The technical assistance by A.-M. Krause was most helpful.

References and Notes

- (1) Koo, J.-Y.; Schuster, G. B. *J. Am. Chem. Soc.* **1977**, *99*, 6107–6109.
- (2) Koo, J.-Y.; Schmidt, S. P.; Schuster, G. B. *Proc. Natl. Acad. Sci. U.S.A.* **1978**, *75*, 30–33.
- (3) Adam, W.; Cueto, O. *J. Am. Chem. Soc.* **1979**, *101*, 6511–6115.
- (4) Adam, W.; Zinner, K.; Krebs, A.; Schmalstieg, H. *Tetrahedron Lett.* **1981**, *22*, 4567–4570.
- (5) Adam, W.; Reinhardt, D.; Saha-Möller, C. R. *Analyst* **1996**, *121*, 1527–1531.
- (6) Beck, S.; Köster, H. *Anal. Chem.* **1990**, *62*, 2258–2270.
- (7) (a) Bronstein, I.; Edwards, B.; Voyta, J. C. *J. Biolumin. Chemilumin.* **1988**, *2*, 186. (b) Edwards, B.; Sparks, A.; Voyta, J. C.; Bronstein, I. *J. Biolumin. Chemilumin.* **1990**, *5*, 1–4. (c) Bronstein, I.; Edwards, B.; Voyta, J. C. *J. Biolumin. Chemilumin.* **1989**, *4*, 99–111. (d) Edwards, B.; Sparks, A.; Voyta, J. C.; Strong, R.; Murphy, O.; Bronstein, I. *J. Org. Chem.* **1990**, *55*, 6225–6229.
- (8) (a) Schaap, A. P.; Chen, T.-S.; Handley, R. S.; DeSilva, R.; Giri, B. P. *Tetrahedron Lett.* **1987**, *28*, 1155–1158. (b) Schaap, A. P.; Handley, R. S.; Giri, B. P. *Tetrahedron Lett.* **1987**, *28*, 935–938.
- (9) Trofimov, A. V.; Mielke, K.; Vasil'ev, R. F.; Adam, W. *Photochem. Photobiol.* **1996**, *63*, 463–467.
- (10) Adam, W.; Bronstein, I.; Edwards, B.; Engel, T.; Reinhardt, D.; Schneider, F. W.; Trofimov, A. V.; Vasil'ev, R. F. *J. Am. Chem. Soc.* **1996**, *118*, 10400–10407.
- (11) Nakamura, H.; Goto, T. *Photochem. Photobiol.* **1979**, *30*, 27–33.
- (12) Koo, J.-Y.; Schuster, G. B. *J. Am. Chem. Soc.* **1978**, *100*, 4496–4503.
- (13) McCapra, F. *Tetrahedron Lett.* **1993**, 6941–6944.
- (14) Matsumoto, M.; Watanabe, N.; Kobayashi, H.; Azami, M.; Ikawa, H. *Tetrahedron Lett.* **1997**, *38*, 411–414.
- (15) Vandereecken, P.; Soumillion, J. Ph.; Van Der Auweraer, M.; De Schryever, F. C. *Chem. Phys. Lett.* **1987**, *136*, 441–446.
- (16) Soumillion, J. Ph.; Vandereecken, P.; Van Der Auweraer, M.; De Schryever, F. C.; Schanck, A. *J. Am. Chem. Soc.* **1989**, *111*, 2217–2225.
- (17) Legros, B.; Vandereecken, P.; Soumillion, J. Ph. *J. Phys. Chem.* **1991**, *95*, 4761–4765.
- (18) Schulz, M. Dissertation, University of Würzburg, Germany, 1993.
- (19) Bronstein, I.; Edwards, B. U.S. Patent No. 5,177,241, 1993.
- (20) Dawson, W. R.; Windsor, M. W. *J. Phys. Chem.* **1968**, *72*, 3251–3260.
- (21) Dewar, M. J. S.; Zoebisch, E. G.; Healy, E. F.; Stewart, J. J. P. *J. Am. Chem. Soc.* **1985**, *107*, 3902–3909.
- (22) Rauhut, G.; Chandrasekhar, J.; Alex, A.; Steinke, T.; Clark, T. *VAMP 5.0*; University of Erlangen-Nürnberg, Germany, 1993.
- (23) Clark, T. Semiempirical molecular orbital theory: facts, myths and legends. In *Recent Experimental and Computational Advances in Molecular Spectroscopy*; Fausto, R., Ed.; Kluwer Academic Publishers: Norwell, MA, 1993; pp 369–380.
- (24) Park, S. M.; Paffett, M. T.; Daub, G. H. *J. Am. Chem. Soc.* **1977**, *99*, 5393–5399.
- (25) Panda, M.; Behera, P. K.; Mishra, B. K.; Behera, G. B. *Indian J. Chem. Sec. A* **1995**, *34*, 11–14.
- (26) Harris, C. M.; Selinger, B. K. *J. Phys. Chem.* **1980**, *84*, 1366–1371.
- (27) Tsutsumi, K.; Shizuka, H. *Z. Phys. Chem.* **1980**, *122*, 129–142.
- (28) Lee, J.; Robinson, G. W.; Webb, S. P.; Phillips, L. A.; Clark, J. H. *J. Am. Chem. Soc.* **1986**, *108*, 6538–6542.